

Development of an Integrated Optofluidic Platform for Droplet and Micro Particle Sensing

Microflow Analyzer for Interrogating Self Aligned Droplets and Droplet Encapsulated Micro Objects

P. K. Shivhare^{1,2}, A. Prabhakar¹ and A. K. Sen²

¹Department of Electrical Engineering, Indian Institute of Technology Madras, Chennai, India

²Department of Mechanical Engineering, Indian Institute of Technology Madras, Chennai, India

Keywords: Optofluidics, Microfluidics, Microflow Cytometry, Droplet Microfluidics, Microflow Analyser, Optical Sensing, Single Cell Analysis, Emulsion, Scattered Signals, Fluorescence Detection, 3D Flow Focusing.

Abstract: Here we report the development of a micro flow analyser that integrates digital microfluidics technology with optoelectronics for the detection of micron size droplets and particles. Digital microfluidics is employed for the encapsulation of microparticles inside droplets that self-align at the centre of a microchannel thus eliminates the need of complicated 3D focusing. Optoelectronics comprise a laser source and detectors for the measurement of forward scatter (FSC), side scatter (SSC) and fluorescence (FL) signals from the microparticles. The optoelectronics was first used with a simple 2D flow focusing channel to detect microparticles which showed uncertainty in the data due to lack of 3D focusing. The integrated device with digital microfluidics technology and optoelectronics was then used for the enumeration and detection of Rhodamine droplets of different size. Rhodamine droplets of different size were characterized based on FSC, SSC and FL. Finally, the device was used for the detection of fluorescent microbeads encapsulated inside aqueous droplets.

1 INTRODUCTION

Integrated optical detection in a microfluidic platform recently got an immense attention, and a new field of study “Optofluidics” have emerged. On such integrated platforms light and fluids are engineered synergistically to implement a highly sensitive and portable lab-on-chip bio-chemical sensors (Psaltis et al. 2006; Testa et al. 2015). Innumerable integrated optofluidic platforms were successfully demonstrated in last few years for various applications for instance, controlling liquid motion using light (Baigl 2012), sunlight based fuel-production (Erickson et al. 2011), microfabrication (Koh et al. 2015), and flow cytometry (Godin et al. 2008). In particular development of portable and economical microflow cytometer is urgently required for addressing the feeble diagnostic situations in rural areas of developing countries. Various microflow analysers were developed for different applications including counting and studying biological cells (Zhang et al.), bacteria (Verborg et al. 2013), cellular DNA

(Ornatsky et al. 2008) droplets (Kunstmann-Olsen et al. 2016).

Isolating and interrogating a micro-object from bulk revealed that the differences in the micro objects and biological cells exists due to the various natural random processes (Xie et al. 2015). Traditional methods, which involves measurement of the probability distribution from a large population ensemble of micro objects may prove to be misleading (Carlo and Lee 2006; Huang et al. 2014) since such study camouflages the unique behaviour of the individual micro objects (Yang et al. 2016a). The study and detection of this particularity may prove to be helpful in early diagnosis of diseases like cancer (Yang et al. 2016b), drug screening (Espulgar et al. 2015), cellular drug metabolism (Chen et al. 2016), intracellular communication (Liu and Lin 2016), etc.

It is known from literature that Water in Oil (W/O) or Oil in Water (O/W) droplets tends to move toward the region with zero shear rate (Leal 1980), this property can be exploited for eliminating the need

of 3D flow focusing in microchannel for the development of a microflow analyser. In addition, ability of microfluidic platforms to manipulate small volumes of fluids (\sim fL to \sim nL) by efficiently producing monodisperse droplets at very high speed (kHz to MHz) makes it an ideal platform for single particle analysis (Martino and Andrew 2016). Miniaturization of traditional test tube into a monodisperse droplet (Kintses et al. 2010) of few micron size not only drastically decreases the volume of sample required for analysis but also efficiently compartmentalizes a particle for various single particle analysis (Joensson and Andersson Svahn 2012). In addition recent developments in the field of digital microfluidics (Jebrail and Wheeler 2010) have equipped the researchers with a complete toolbox for droplet manipulation which includes various functional operations such as sorting, splitting, mixing, incubation of droplets (Kintses et al. 2010).

Nevertheless, challenges exist in realizing a commercially viable product. The main hindrance in the development of a microflow analyser are complicated techniques required for 3D flow focusing of sample and the control of interdistance between the micro particles in order to avoid presence of multiple objects in the optical window. (Shivhare et al. 2016). Similarly, several challenges are present for single particle analysis in terms of increasing throughput, ultra-sensitive detection of extremely small volume (Xie et al. 2015; Yang et al. 2016b), and dynamic control of environment (Carlo and Lee 2006) for such measurement. Techniques such as microdissection and micromanipulators are presently employed for single particle analysis. However, these methods require complex manipulations (Xie et al. 2015) and in addition costly equipments further limit availability of these techniques. Further, the optical detection of micro particle encapsulated inside droplet was not paid any attention. Thus, techniques for isolation and cost-effective detection of single micro particle from bulk are urgently required.

In this work, we report the development of an integrated optofluidic microflow analyser for non-invasive optical detection of 2D-focused micro particle. The inherent property of droplets to move toward region with zero shear rate is employed for generating self-aligned droplets thereby eliminating the need of complicated 3D flow focusing mechanisms. Forward scattered (FSC), side scattered (SSC) and fluorescent (FL) signals are collected and mapped in a scatter plot. Further, the platform is also used for isolating and sensing of single micro objects by trapping the object in the discrete droplet surrounded by an immiscible phase.

2 EXPERIMENTS

2.1 Design and Microfabrication

Figure 1 shows image of the integrated optofluidic device used for interrogating 2D flow focused polystyrene beads, droplets, droplet generation rate, and measurement of FSC, SSC, and FL from a droplet encapsulated polystyrene fluorescent beads. The device is incorporated with an on-chip droplet generator to generate droplets and facilitate compartmentalization of single micro particle for optical interrogation. In all experiments the sample (mostly aqueous phase) was infused using sample inlet while continuous phase (mostly oil phase) was infused through sheath inlet. As marked, the device is equipped with four grooves for embedding an in-situ optical detection zone by inserting optical fiber. Groove 1 was used to illuminate the sample using a lensed fiber to focus the laser beam to a spot of $10\ \mu\text{m}$ in the center of microchannel, whereas fibers in Groove 2, Groove 3, and Groove 4 were placed at 5° anticlockwise, 45° clockwise, and 135° clockwise with respect to incident beam and used to obtain FSC, SSC, and FL signals respectively.

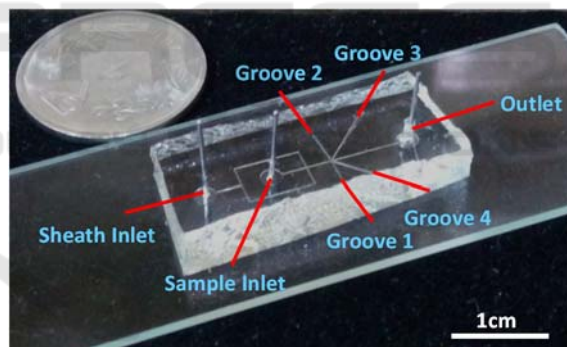


Figure 1: Image of the integrated optofluidics device employed for the measurements.

The design of the device was made using CAD software (Autodesk® AutoCAD 2015) and clear field photomask was printed with the resolution of 40000 dpi. Finally, Polydimethylsiloxane (PDMS) based microfluidic device was obtained employing standard photolithography technique followed by soft lithography process, a detailed description of the process is provided in the literature (Sajeesh et al. 2014). In order to insert standard available multimode $62.5/125\ \mu\text{m}$ optical fiber, the depth of the device was kept at $130\ \mu\text{m}$. The width of the main fluid channel and throat of droplet generator junction were $100\ \mu\text{m}$ and $30\ \mu\text{m}$ respectively.

2.2 Materials and Methods

2.2.1 Aqueous and Oil Phases

Deionized (DI) water mixed with varying concentrations of Rhodamine Dye (Sigma Aldrich, Bangalore, India) was used as discrete phase while olive oil (Sigma Aldrich, Bangalore, India) was used as continuous phase in the experiments. First, a highly concentrated 52.19 mM Rhodamine solution was prepared by adding 100mg of Rhodamine B (Sigma Aldrich, Bangalore) dye in 4mL of aqueous glycerol solution (22% wt/wt). Now this concentrated solution was further diluted to get 130 μ M solution. Aqueous Rhodamine solution and olive oil were filtered with 0.2 μ m PTFE and nylon filters respectively (Axiva Sicheem Biotech, Chennai, India) to avoid clogging due to unsolicited dust in the microfluidic channel. In order to stabilize the droplets, 5% wt/wt of Tween 80 (Sigma Aldrich Bangalore, India) was added to the Rhodamine solution as surfactant.

2.2.2 Microbeads

Fluorescent polystyrene beads (Sigma Aldrich Bangalore, India) of diameter 10 μ m and 15 μ m was mixed in aqueous glycerol solution (22% wt/wt) in order to avoid sedimentation of beads. 0.5% wt/wt of surfactant Tween 80 (Sigma Aldrich Bangalore, India) was added to the solution to prevent the aggregation of the beads present in the solution. The original bead solution was diluted with the aqueous solution.

2.3 Optical Sensing Setup

A block diagram of optical detection system incorporated for measurements is shown in Fig. 2. Graded index multimode (62.5/125 μ m) fiber coupled 20mW, 532 nm turnkey laser system (VTEC Lasers and Sensors, The Netherlands) was employed for illuminating the sample (Using Groove

1). The FSC data was collected using Si PIN photodiode (DET02AFC/M, Thorlabs Inc., USA), whereas for collecting feeble SSC and FL signal highly sensitive Si semiconductor based avalanche photodiode (C10508-01, Hamamatsu Photonics, Japan) and single photon counting module (SPCM50A/M, Thorlabs Inc., USA) are used respectively, as compared to traditional slower and bulky photomultiplier tubes (PMT). The use of smaller semiconductor detectors increases portability of the system. All these detectors were connected to the microfluidic chip using multimode fibers (62.5/125 μ m) inserted in the fiber grooves as explained in Section 2.1 of the manuscript. An optical band pass filter at 575/50 nm (ET575/50m, Chroma Technology Corp., USA) was attached to single photon counting module (SPCM) to filter out the illuminating wavelength of 532 nm and measure fluorescence signal.

The FSC and SSC signals were sampled at 10kHz while FL signal was sampled at 5kHz. The data was collected using data acquisition system (NI-USB-6251, National Instruments, India) and in-house software written in LabVIEW®. Data was analysed on a computer using an in-house built Python software to obtain width, amplitude, and area for each pulse (each particle/droplet crossing the detection region).

2.4 Experimental Setup

Pressure based pumping system (MFCS-EZ, Fluigent SA, France) were used to infuse the fluids into the microchannels. Inverted microscope (Axiovert A1, Carl Zeiss GmbH, Germany) attached with high speed camera (SA3, Phoron, USA) was used to capture the videos at 1000 frames. ImageJ (Rasband, W. S., ImageJ, USA) was used to analyse the videos to obtain the droplet generation rate (f_d), and droplet diameter (d_d).

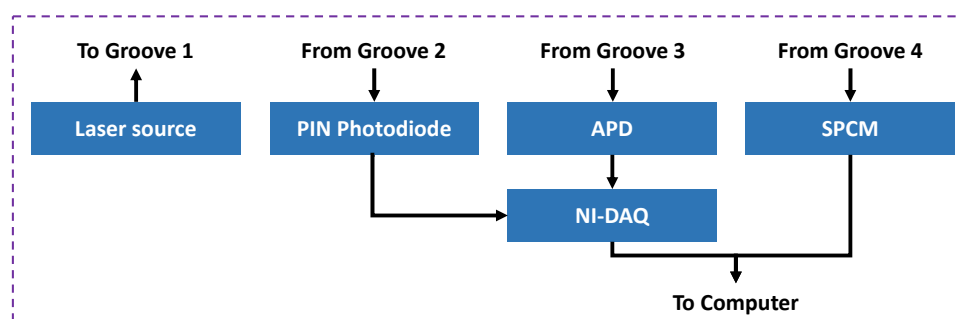


Figure 2: Block diagram of the optical detection system.

3 RESULTS AND DISCUSSION

3.1 2-D focused Micro Particles

Microbeads solution and DI water were infused in the microchannel from sample and sheath inlet respectively. The focused streams of microbeads were passed through detection region and FSC of each event was obtained. Fig. 3(a) shows the scatter plot of scattered signal v_{FSC} vs. residence time τ (pulse-width) for large number of beads passing through detection region. Fig. 3(b) represents the normalized distribution of the scattered signal v_{FSC} for micro particles of 10 μm and 15 μm , data was fit to normal distribution with R^2 value of 0.87 and 0.79 respectively. It can be clearly observed that micro particles of different sizes form different colonies in the scatter plot marked with ellipses in Fig. 3(a).

Remark that residence time of beads of different sizes are comparable, this is attributed to the fact that the beads are focused only in horizontal plane and are free to move in any vertical plane. Since, mobility (Sajeesh et al. 2014) profile is parabolic along the vertical plane (Shivhare et al. 2016), particle along center line requires less time to traverse detection region, as compared to the particle travelling near the wall. The scattered signal v_{FSC} is proportional to size of micro particle crossing the detection region (Cho et al. 2010), and thus the amplitude of scattered signal in case of bigger beads is higher than smaller beads as can be observed from Fig. 3(a). This can also be observed from Fig. 3(b), where mean value of signal for normal distribution corresponding to 15 μm is higher than 10 μm . However, we can clearly notice the presence of 10 μm particles in the colony of 15 μm

and vice versa. This is due to the fact that since the particles are focused in only horizontal plane multiple beads can pass the detection region at the same instant which introduces the error in the measurement (Shivhare et al. 2016). Thus 2D focused micro particles of varying sizes can be segregated with FSC signal, however, varying mobility in the vertical plane and presence of multiple particles in the detection region introduce error in the measurement. This error introduced due to the variation of mobility can be eliminated by focusing the particle from all direction. Thus 3D flow focusing is required for sensitive cytometric application.

3.2 Rhodamine Droplets

Continuous stream of Rhodamine water droplets were generated with olive oil as continuous phase and rhodamine dye solution as discrete phase. The size of the droplets was varied by varying the pressure of continuous and discrete phases. FSC, SSC, and FL were measured for these droplets. Figure 4 shows the signal collected from a train of droplets crossing the microchannel. It can be observed from the data that as the droplet passes the detection zone it hinders the path of continuous beam of laser light and scatters the light in various direction which results in pulse in scattered signals. Note that when droplet passes the detection zone FSC encounters a negative pulse due to the obstruction of continuous beam of light. This light gets scattered in different direction due to interface between droplet and continuous phase which results in positive pulse in SSC. Also since droplet is devised using fluorescent dye, a pulse in FL signal is captured by SPCM as droplet crosses the detection zone.

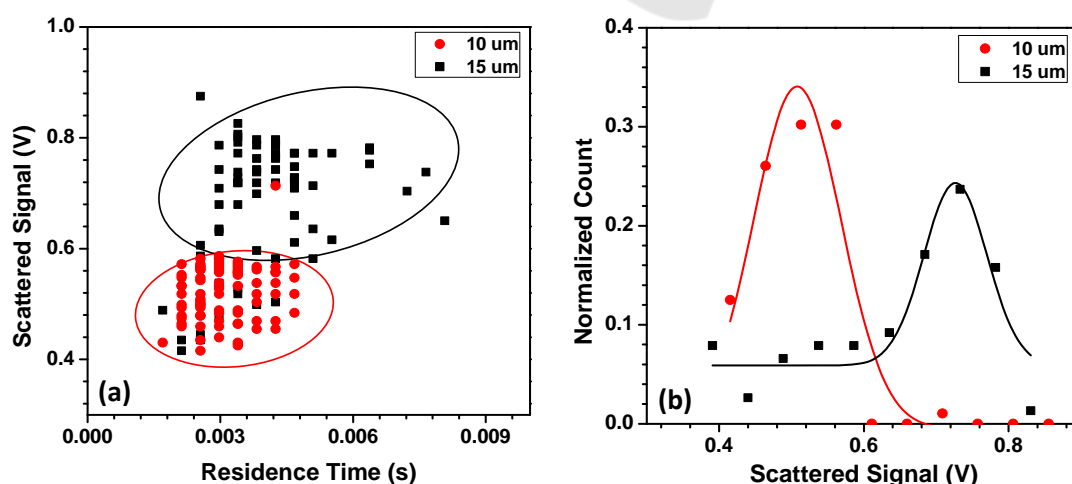


Figure 3: (a) Scatter plot of Scattered Signal (v_{FSC}) vs. Residence Time (τ) (b) Normalized distribution of scattered signal v_{FSC} for 2D focused micro particles of sizes 10 μm and 15 μm .

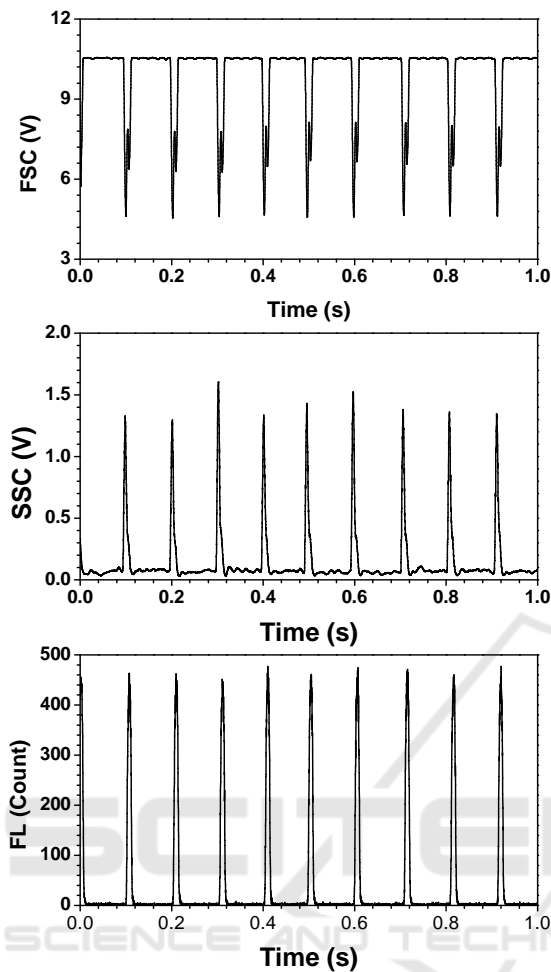


Figure 4: FSC, SSC, and FL data from a stream of continuous Rhodamine droplet.

Figure 5(a) illustrates the images of the Rhodamine droplets generated in the microchannel, whereas Figure 5(b) represents the 3D scatter plot of FSC-SSC-FL signal of each droplet passing the detection zone from droplet of varying sizes. The size (in μm) of the corresponding droplets is mentioned as legend in the figure and scale on all images in Figure 5(a) represents $100\mu\text{m}$. It can be observed from the Figure 5(b) that droplets of different sizes form the different colony in the scatter plot.

Droplets in microfluidic channel tends to move towards the region with zero shear rate due to the deformability induced lift forces (Leal 1980). In the present design, due to symmetric flow conditions the region with zero shear rate tends to be the centreline of the microchannel which results in self 3D flow focusing of the interrogated objects. Thus this self-alignment of droplets eliminated the need of complex 3D flow focusing setup (Shivhare et al. 2016) and

hence need of extra bulky pumping system required. This improves the portability of the system and also makes it relatively less complex.

The impact of this 3D flow focusing is clearly visible in the scattered plot (Figure 5(b)) where the various colonies are well separated as compared to the 2D focused micro particles as shown in Figure 3 (b). This distinction in the colonies is critical for measurement of properties like size, type, velocity of the object. Thus the use of droplets as the miniaturized test tube in the cytometric applications reduces the error due to mobility variation of micro particles.

The other important concern in the cytometric measurement is the control of minimum interdistance between the particles in order to avoid the multiple objects in the optical window (Shivhare et al. 2016). This issue can also be addressed using droplet microfluidics since the droplet generation rate can be controlled using flow rate of discrete and continuous phase (Nguyen et al. 2006).

3.3 Particle Encapsulation

The polystyrene beads were compartmentalized in the water in oil (W/O) droplets with Olive oil as continuous phase and microbeads solution described in the Section 2.2.2 as discrete phase. As droplets are generated a bead present in the solution gets trapped inside the droplet, and thus gets completely isolated from the rest of beads (bulk). Now using the already reported tools for droplet manipulation (Jebrail and Wheeler 2010) various single particle experiments can be performed on the isolated micro particle. The number of positive droplets (droplets containing a micro particle) can be increased by increasing the concentration of the micro particle. The relation between the numbers of micro-particles in the droplet is given by Poisson's distribution $P(x) = \frac{\exp(-\lambda) \times \lambda^x}{x!}$, where $P(x)$ represents the probability of presence of x beads in a droplet with λ representing mean number of beads in the volume of each droplet (Mazutis et al. 2013). Thus, as the concentration of bead in the solution increases, droplets containing multiple particle, also increases. (Chabert and Viovy 2008).

Figure 6(a) and Figure 6(b) represents the image of a negative (droplet without micro particle) and positive droplets (droplet with micro particle) respectively. It can be clearly perceived from the image that Figure 6(b) contains a micro particle. Figure 6 (c), (d), and (e) shows the FSC, SSC, and FL data captured from the stream of mixture of positive and negative droplet crossing the detection zone. The

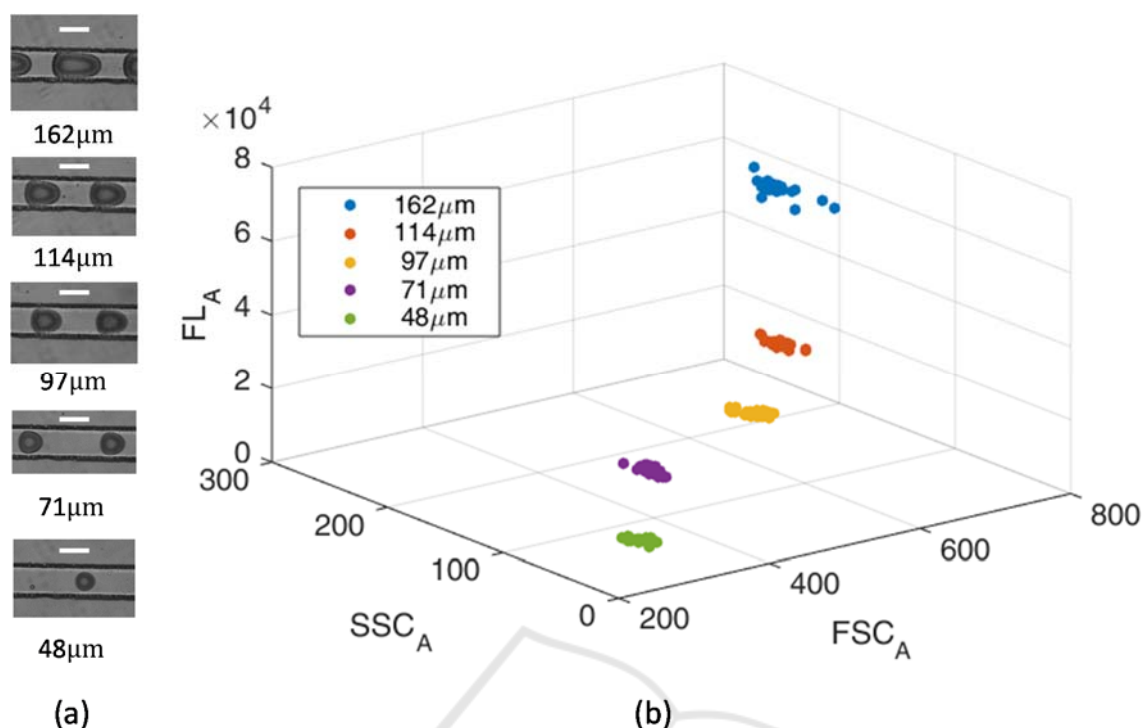


Figure 5: (a) Images of droplets of varying sizes flowing inside the microchannel (b) 3D scatter plot of FSC-SSC-FL signal from Rhodamine droplets of varying sizes.

dashed rectangle (8th and 9th pulse) in the graph are the positive droplets, while other pulses are from negative droplets. It can be observed from the Figure 6(c) that the FSC of positive (8th and 9th pulse) and negative droplets (except 8th and 9th pulse) are almost similar, this is attributed to the fact that the FSC signal is proportional to the size of droplets which remains unaltered for positive and negative droplets. However, SSC is proportional to the internal granularity of the object which is being interrogated. Since, the positive droplet contains the micro particle the internal structure of these droplets differ from negative ones, this change in the granularity can clearly be observed in the SSC signal shown in Figure 6(d). Note that positive droplets (8th and 9th pulse) possess two peaks as compared to the single peak in negative droplets. This is further confirmed by the FL signal shown in Figure 6(e) where peaks are present only for the droplets containing fluorescent beads.

The developed integrated platform simultaneously exploits the advancements in the field of digital microfluidics and optofluidics for isolating a particle from bulk and real time non-invasive optical interrogation. Further, sorting mechanism can be employed to separate and collect the positive droplets for further analysis. This device provides a low cost alternative to the presently employed

complex techniques for single particle analysis.

4 CONCLUSIONS

In this work, we reported the development of an integrated optofluidic microflow analyser which consists of a microfluidic channel and a set of optical fiber grooves for simultaneous measurement of various scattered signal viz. FSC, SSC, and FL signal. An optical illumination and detection system comprising of green laser source, Si PIN photodiode, Si avalanche photodiode, and Single Counting Photon Module was designed. Polystyrene beads of 10 μm and 15 μm were focused in horizontal plane (two dimensional focusing) and scattered signals were collected. The obtained scatter plot shows that error in the measurement is introduced due to the variation in mobility of particles and presence of multiple objects in the optical detection window since particles were not focused in vertical plane. Both of these error, which are measure concern for the development of microflow analyser, were eliminated with the formulation of self-focused droplet inside the microchannel. The collected scattered signals formed the distinct colonies for droplet of varying sizes on the scatter plot, which is critical for various

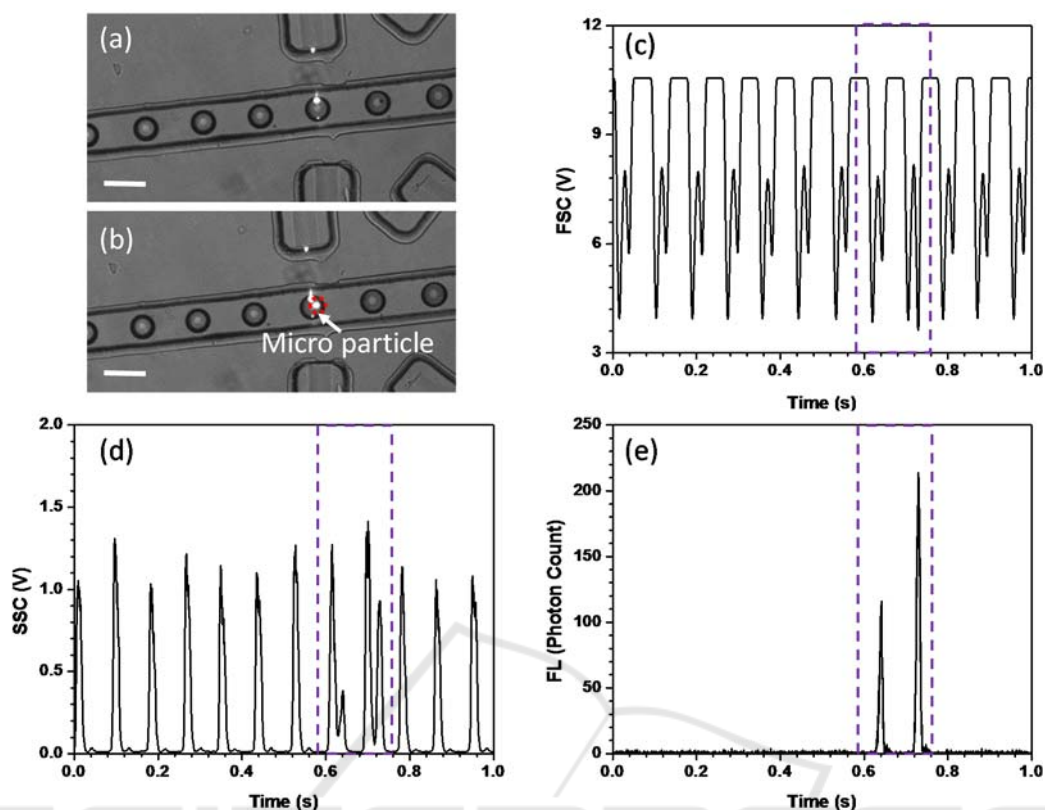


Figure 6: (a) Image of droplet without micro particle (b) Image of droplet with micro particle (c) FSC (d) SSC (e) FL signal from a stream of mixture of positive and negative droplets in the microchannel.

cytometric measurements. Finally the proof of concept was demonstrated for single particle analysis by encapsulating and optically interrogating $10\mu\text{m}$ fluorescent polystyrene beads inside the droplet.

Also, the use of droplets to compartmentalize the micro particles drastically reduced the volume of sample required. Thus the developed platform incorporating droplets encapsulation of micro particle and optical interrogation can prove to be low cost, portable, non-invasive alternative for single particle analysis.

ACKNOWLEDGEMENTS

The authors would like to thank SERB, DST (Project No. MEE/15-16/340/DSTXASHS) and IIT Madras for providing financial support for the project. We acknowledge support of Centre of NEMS and Nanophotonics (CNNP), IIT Madras with the photolithography work. Also, we thank the Interdisciplinary Research Program, IIT Madras, which enabled this work.

REFERENCES

- Baigl D (2012) Photo-actuation of liquids for light-driven microfluidics: state of the art and perspectives. *Lab Chip* 12:3637. doi: 10.1039/c2lc40596b.
- Carlo D Di, Lee LP (2006) Dynamic Single-Cell Analysis for Quantitative Biology. *Anal Chem* 78:7918–7925. doi: DOI: 10.1021/ac069490p.
- Chabert M, Viovy J-L (2008) Microfluidic high-throughput encapsulation and hydrodynamic self-sorting of single cells. *Proc Natl Acad Sci U S A* 105:3191–3196. doi: 10.1073/pnas.0708321105.
- Chen F, Lin L, Zhang J, et al (2016) Single-Cell Analysis Using Drop-on-Demand Inkjet Printing and Probe Electrospray Ionization Mass Spectrometry. *Anal Chem* 88:4354–4360. doi: 10.1021/acs.analchem.5b04749.
- Cho SH, Godin JM, Chen C-H, et al (2010) Review Article: Recent advancements in optofluidic flow cytometer. *Biomicrofluidics*. doi: http://dx.doi.org/10.1063/1.3511706.
- Erickson D, Sinton D, Psaltis D (2011) Optofluidics for energy applications. *Nat Photonics* 5:583–590. doi: 10.1038/nphoton.2011.209.
- Espulgar W, Yamaguchi Y, Aoki W, et al (2015) Single cell trapping and cell-cell interaction monitoring of

- cardiomyocytes in a designed microfluidic chip. *Sensors Actuators, B Chem* 207:43–50. doi: 10.1016/j.snb.2014.09.068.
- Godin J, Chen CH, Cho SH, et al (2008) Microfluidics and photonics for bio-System-on-a-Chip: A review of advancements in technology towards a microfluidic flow cytometry chip. *J Biophotonics* 1:355–376. doi: 10.1002/jbio.200810018.
- Huang N-T, Zhang H-L, Chung M-T, et al (2014) Recent advancements in optofluidics-based single-cell analysis: optical on-chip cellular manipulation, treatment, and property detection. *Lab Chip* 14:1230–1245. doi: 10.1039/c3lc51211h.
- Jebrail MJ, Wheeler AR (2010) Let's get digital: Digitizing chemical biology with microfluidics. *Curr Opin Chem Biol* 14:574–581. doi: 10.1016/j.cbpa.2010.06.187.
- Joansson HN, Andersson Svahn H (2012) Droplet microfluidics-A tool for single-cell analysis. *Angew Chemie - Int Ed* 51:12176–12192. doi: 10.1002/anie.201200460.
- Kintses B, van Vliet LD, Devenish SRA, Hollfelder F (2010) Microfluidic droplets: New integrated workflows for biological experiments. *Curr Opin Chem Biol* 14:548–555. doi: 10.1016/j.cbpa.2010.08.013.
- Koh J, Wu C-Y, Kittur H, Di Carlo D (2015) Research highlights: microfluidically-fabricated materials. *Lab Chip* 15:3818–3821. doi: 10.1039/C5LC90092A.
- Kunstmann-Olsen C, Hanczyc MM, Hoyland J, et al (2016) Uniform droplet splitting and detection using Lab-on-Chip flow cytometry on a microfluidic PDMS device. *Sensors Actuators B Chem* 229:7–13. doi: 10.1016/j.snb.2016.01.120.
- Leal LG (1980) Particle Motions in a Viscous Fluid. *Annu Rev Fluid Mech* 12:435–76.
- Liu W, Lin J-M (2016) Online Monitoring of Lactate Efflux by Multi-Channel Microfluidic Chip-Mass Spectrometry for Rapid Drug Evaluation. *ACS Sensors* 1:500221. doi: 10.1021/acssensors.5b00221.
- Martino C, Andrew J (2016) Droplet-based microfluidics for artificial cell generation: a brief review. doi: 10.1098/rsfs.2016.0011.
- Mazutis L, Gilbert J, Ung WL, et al (2013) Single-cell analysis and sorting using droplet-based microfluidics. *Nat Protoc* 8:870–891. doi: 10.1038/nprot.2013.046. <http://www.nature.com/nprot/journal/v8/n5/abs/nprot.2013.046.html#supplementary-information>.
- Nguyen NT, Lassemono S, Chollet FA (2006) Optical detection for droplet size control in microfluidic droplet-based analysis systems. *Sensors Actuators, B Chem* 117:431–436. doi: 10.1016/j.snb.2005.12.010.
- Ornatsky OI, Lou X, Nitz M, et al (2008) Study of Cell Antigens and Intracellular DNA by Identification of Element-Containing Labels and Metallointercalators Using Inductively Coupled Plasma Mass Spectrometry proliferation in clinical samples is important for diagnostic. *Anal Chem* 80:2539–2547. doi: 10.1039/b710510j.as.
- Psaltis D, Quake SR, Yang C (2006) Developing optofluidic technology through the fusion of microfluidics and optics. *Nature* 442:381–6. doi: 10.1038/nature05060.
- Sajeesh P, Doble M, Sen AK (2014) Hydrodynamic resistance and mobility of deformable objects in microfluidic channels. *Biomicrofluidics* 8:54112. doi: 10.1063/1.4897332.
- Shivhare PK, Bhadra A, Sajeesh P, et al (2016) Hydrodynamic focusing and interdistance control of particle-laden flow for microflow cytometry. *Microfluid Nanofluidics* 20:86. doi: 10.1007/s10404-016-1752-z.
- Testa G, Persichetti G, Bernini R (2015) Optofluidic approaches for enhanced microsensor performances. *Sensors (Switzerland)* 15:465–484. doi: 10.3390/s150100465.
- Verbarq J, Plath WD, Shriver-Lake LC, et al (2013) Catch and release: Integrated system for multiplexed detection of bacteria. *Anal Chem* 85:4944–4950. doi: 10.1021/ac303801v.
- Xie W, Gao D, Jin F, et al (2015) Study of Phospholipids in Single Cells Using an Integrated Microfluidic Device Combined with Matrix-Assisted Laser Desorption/Ionization Mass Spectrometry. *Anal Chem* 87:7052–7059. doi: 10.1021/acs.analchem.5b00010.
- Yang M, Nelson R, Ros A (2016a) Toward Analysis of Proteins in Single Cells: A Quantitative Approach Employing Isobaric Tags with MALDI Mass Spectrometry Realized with a Microfluidic Platform. *Anal Chem* 88:6672–6679. doi: 10.1021/acs.analchem.5b03419.
- Yang T, Gao D, Jin F, et al (2016b) Surface-printed microdot array chips coupled with matrix-assisted laser desorption/ionization mass spectrometry for high-throughput single-cell patterning and phospholipid analysis. *Rapid Commun Mass Spectrom* 30:73–79. doi: 10.1002/rcm.7628.
- Zhang Y, Watts BR, Guo T, et al Optofluidic Device Based Microflow Cytometers for Particle / Cell Detection : A Review. 1–21. doi: 10.3390/mi7040070.